

Phase Diagram of Cold Polarized Fermi Gas in Two Dimensions

Lianyi He and Pengfei Zhuang

Physics Department, Tsinghua University, Beijing 100084, China

The superfluid phase diagrams of a two-dimensional cold polarized Fermi gas in the BCS-BEC crossover are systematically and analytically investigated. In the BCS-Leggett mean field theory, the transition from unpolarized superfluid phase to normal phase is always of first order. For a homogeneous system, the two critical Zeeman fields and the critical population imbalance are analytically determined in the whole coupling parameter region, and the superfluid-normal mixed phase is shown to be the ground state between the two critical fields. The density profile in the presence of a harmonic trap calculated in the local density approximation exhibits a shell structure, a superfluid core at the center and a normal shell outside. For weak interaction, the normal shell contains a partially polarized cloud with constant density difference surrounded by a fully polarized state. For strong interaction, the normal shell is totally in fully polarized state with a density profile depending only on the global population imbalance. The di-fermion bound states can survive in the whole highly imbalanced normal phase.

PACS numbers: 03.75.Ss, 05.30.Fk, 74.20.Fg, 34.90.+q

I. INTRODUCTION

The effect of Zeeman energy splitting h induced by a strong magnetic field between spin up and down electrons on Bardeen-Cooper-Schrieffer (BCS) superconductivity, which has been investigated many years ago [1, 2, 3], promoted new interest in recent years due to the progress in the experiments of ultracold Fermi gases [4, 5, 6, 7, 8, 9]. The well-known result for weak-coupling s-wave superconductivity is that, at a critical Zeeman field or the so-called Chandrasekhar-Clogston (CC) limit $h_c = 0.707\Delta_0$ where Δ_0 is the zero temperature gap, the Cooper pairs are destroyed and a first order quantum phase transition from the gapped BCS state to the normal state occurs [1]. Further studies showed that the inhomogeneous Fulde-Ferrell-Larkin-Ovchinnikov (FFLO) state [3] where Cooper pairs have nonzero momentum can survive above the CC limit up to $h_{\text{FFLO}} = 0.754\Delta_0$. However, since the thermodynamic critical field is much smaller than the CC limit due to strong orbit effect [1], it is hard to observe the CC limit and the FFLO state in ordinary superconductors.

Recent experiments on ultracold Fermi gas trapped in an external harmonic potential, serve as an alternative way to study the pure Zeeman effect on Fermi superfluidity [4, 5, 6, 7, 8, 9]. The atom numbers of the two lowest hyperfine states of ^6Li atom, N_\uparrow and N_\downarrow , are adjusted to create a population imbalance or polarization $P = (N_\uparrow - N_\downarrow)/(N_\uparrow + N_\downarrow)$, which simulates the Zeeman field h in a superconductor. The s-wave attraction between the two hyperfine states is tuned around the Feshbach resonance to realize a strongly rather than weakly interacting Fermi gas. In three-dimensional case, the density profiles observed in experiments exhibit an unpolarized superfluid core in the center of the trap and a polarized normal gas shell outside [4, 5, 6, 7], which justifies that the ground state around unitary is a phase separation state (although there may be some dispute on the shell structure), predicted by early theoretical

works [10, 11, 12, 13, 14].

One of the theoretical interests in the study of polarized Fermi superfluidity is to determine its phase structure in the whole interaction strength region, namely in the BCS-BEC (Bose-Einstein Condensation) crossover [13, 14]. The complete mean field phase diagram in coupling-imbalance plane as well as the critical Zeeman field h_c and critical polarization P_c are theoretically predicted in three dimensional case (3D) [13]. Since the s-wave mean field equations can not be solved analytically in the whole coupling region, it is hard to determine a precise phase diagram in 3D even in mean field approximation. Recently, the quantitatively correct phase diagram in 3D has been obtained in quantum Monte Carlo calculations [15, 16]. However, the theoretical prediction of the phase diagram for a homogeneous system can not be directly examined in ultracold Fermi gas experiments, due to the effect of the external harmonic trap. To have a comparison with the experimental data, one should investigate the phase diagram and the density profile in the presence of an external trap potential, using the same equation of state. In the case of 3D, the density profile can only be treated numerically [17].

While we have well understood the 3D phase diagram, the phase structure of polarized Fermi gases in low dimensions promoted recently experimental and theoretical interests. In one dimensional case the phase diagram is determined via exact solvable models [18]. In the two-dimensional case, while exact solvable models are lacked, the s-wave mean field equations can be solved analytically in the whole coupling parameter region [19, 20, 21, 22], and the Fermi surface topology and stability condition are not trivial and different from those in 3D [23]. In this paper, we will determine the phase diagrams of a polarized Fermi gas in two dimensions, for both homogeneous and trapped systems, and calculate the density profile of a trapped imbalance Fermi gas. Our results are totally analytical in the whole coupling parameter region, including the phase diagrams and the density profile. In

the final part of this paper, we also discuss the existence of di-fermion bound states in the polarized normal phase.

II. BCS-BEC CROSSOVER IN TWO DIMENSIONS

The BCS-BEC crossover problem in two dimensions has been widely discussed in the literatures[19, 20, 21, 22]. In this paper, we employ an effective 2D Hamiltonian where the renormalized atom-atom interaction can be characterized by an effective binding energy[19]. For a wide Feshbach resonance, the effective grand canonical Hamiltonian can be written as

$$H = \sum_{\sigma=\uparrow,\downarrow} \int d^2\mathbf{r} \psi_{\sigma}^{\dagger}(\mathbf{r}) \left(-\frac{\hbar^2}{2M} \nabla^2 - \mu - \sigma_z h \right) \psi_{\sigma}(\mathbf{r}) - U \int d^2\mathbf{r} \psi_{\uparrow}^{\dagger}(\mathbf{r}) \psi_{\downarrow}^{\dagger}(\mathbf{r}) \psi_{\downarrow}(\mathbf{r}) \psi_{\uparrow}(\mathbf{r}), \quad (1)$$

where M is the fermion mass, μ is the chemical potential, $U > 0$ is the contact attractive interaction, and $\sigma_z = \pm 1$ correspond to $\sigma = \uparrow, \downarrow$. We choose the unit $\hbar = 1$ through the paper. The Zeeman field h can be created by either an external field[1, 2, 3] or a population imbalance[4, 5]. In the former case, the total particle number N is conserved, but the particles N_{\uparrow} and N_{\downarrow} in the states \uparrow and \downarrow can transfer to each other[24], i.e., the chemical potentials for the two components are always the same, but the external field h induces an effective chemical potential difference. In the latter case, N_{\uparrow} and N_{\downarrow} are both conserved, and the two chemical potentials can be expressed as $\mu_{\uparrow} = \mu + h$ and $\mu_{\downarrow} = \mu - h$.

At finite temperature in 2D, the long range order is absent and no phase transition can happen. At zero temperature, however, there do exist long range order [22] and one can safely consider phase transitions among different states. In this paper, we will study the phase diagrams at zero temperature in the BCS-Leggett mean field approximation which is accepted to adequately describe the BCS-BEC crossover at $T = 0$ [25].

In the balanced case with $h = 0$, the thermodynamic potential density of a uniform Fermi gas can be evaluated as[22]

$$\Omega(\mu; \Delta) = \frac{\Delta^2}{U} + \int \frac{d^2\mathbf{k}}{(2\pi)^2} (\xi_{\mathbf{k}} - E_{\mathbf{k}}) \quad (2)$$

with the definition of particle energies $E_{\mathbf{k}} = \sqrt{\xi_{\mathbf{k}}^2 + \Delta^2}$ and $\xi_{\mathbf{k}} = \mathbf{k}^2/(2M) - \mu$ and the superfluid order parameter $\Delta = -U \langle \psi_{\downarrow} \psi_{\uparrow} \rangle$. In the dilute limit, the UV divergence in the expression of Ω can be eliminated via introducing the two body scattering length.

While the two-body bound state in 3D forms only at sufficiently strong attraction where the s-wave scattering length diverges and changes sign, the bound state in 2D can form at any arbitrarily small attraction[26]. For an inter-atomic potential described by a 2D circularly symmetric well of radius R_0 and depth V_0 , the bound-state

energy ϵ_B is given by $\epsilon_B \simeq 1/(2MR_0^2) \exp[-2/(MV_0R_0^2)]$ with $V_0R_0^2 \rightarrow 0$. As a consequence, the solution of the BCS-BEC problem in 2D is much simpler than that in the case of 3D in terms of special functions[20]. It is shown that the existence of the two-body bound state in vacuum is a necessary (and sufficient) condition for the Cooper instability[19]. To regulate the UV divergence in Ω , we introduce a high energy cutoff $\Lambda = \mathbf{k}_{\Lambda}^2/(2M)$ in the integral. The momentum cutoff k_{Λ} corresponds to the inverse of the range r_0 of the interaction potential. Due to the energy independence of the density of states in 2D, after performing the integration over \mathbf{k} one obtains

$$\Omega = \frac{\Delta^2}{U} - \frac{M\Delta^2}{4\pi} \left[\ln \frac{\Lambda - \mu + \sqrt{(\Lambda - \mu)^2 + \Delta^2}}{\sqrt{\mu^2 + \Delta^2} - \mu} + \frac{\Lambda - \mu}{\Lambda - \mu + \sqrt{(\Lambda - \mu)^2 + \Delta^2}} + \frac{\mu}{\sqrt{\mu^2 + \Delta^2} - \mu} \right] \quad (3)$$

In this paper we consider a dilute Fermi gas with effective interaction range $r_0 \rightarrow 0$. Taking large enough cutoff Λ and small enough attraction U , we can introduce a 2D two-body binding energy[22] to replace the cutoff in this limit,

$$\epsilon_B = 2\Lambda \exp\left(-\frac{4\pi}{MU}\right), \quad (4)$$

which does not include any many-particle effect. With the binding energy, the cutoff dependence can be eliminated in the dilute limit with $\Lambda \rightarrow \infty$ and $U \rightarrow 0$ but finite ϵ_B . We obtain in this limit

$$\Omega = \frac{M\Delta^2}{4\pi} \left(\ln \frac{\sqrt{\mu^2 + \Delta^2} - \mu}{\epsilon_B} - \frac{\mu}{\sqrt{\mu^2 + \Delta^2} - \mu} - \frac{1}{2} \right). \quad (5)$$

The above procedure is equivalent to directly substituting the coupling constant U by the 2D bound state equation

$$\frac{1}{U} = \int \frac{d^2\mathbf{k}}{(2\pi)^2} \frac{1}{\mathbf{k}^2/M + \epsilon_B}. \quad (6)$$

The BCS-BEC crossover phenomenon in 2D can be observed by solving the coupled gap and number equations, namely $\partial\Omega/\partial\Delta = 0$ and $n = -\partial\Omega/\partial\mu$. Defining the Fermi energy $\epsilon_F = \pi n/M$ in 2D, the gap and number equation can be analytically expressed as

$$\sqrt{\mu^2 + \Delta^2} - \mu = \epsilon_B, \quad \sqrt{\mu^2 + \Delta^2} + \mu = 2\epsilon_F, \quad (7)$$

respectively. Their solution takes a very simple form[19]

$$\Delta_0 = \sqrt{2\epsilon_B\epsilon_F}, \quad \mu_0 = \epsilon_F - \frac{\epsilon_B}{2}, \quad (8)$$

or rewrite it in terms of a dimensionless quantity $\eta = \epsilon_B/\epsilon_F$,

$$\frac{\Delta_0}{\epsilon_F} = \sqrt{2\eta}, \quad \frac{\mu_0}{\epsilon_F} = 1 - \frac{\eta}{2}. \quad (9)$$

One sees very clear that the chemical potential decreases with increasing coupling or decreasing density, which indicates a BCS-BEC crossover. The Chemical potential changes sign at $\epsilon_B = 2\epsilon_F$. To understand the physical significance of these simple results, we consider two limits. For very weak attraction (or high density), the two-particle binding energy is extremely small, i.e. $\epsilon_B \ll \epsilon_F$, and we recover the well-known BCS result with strongly overlapping Cooper pairs. In this limit we have the chemical potential $\mu_0 \simeq \epsilon_F$ and the gap function $\Delta_0 \ll \epsilon_F$. For the opposite limit of very strong attraction (or low particle density), we have a deep two-body bound state with $\epsilon_B \gg \epsilon_F$, and the system is in the BEC region with composite bosons. In this limit the chemical potential takes $\mu_0 \simeq -\epsilon_B/2$. It should be kept in mind that in the local pair regime ($\mu_0 < 0$) the fermion excitation gap E_{gap} in the quasi-particle excitation spectrum is not Δ_0 (as in the case $\mu_0 > 0$) but rather $\sqrt{\mu_0^2 + \Delta_0^2}$.

In ultracold Fermi gas experiments, a quasi-2D Fermi gas can be realized by arranging a one-dimensional optical lattice along the axial (z) direction and a weak harmonic trapping potential in the radial (x - y) plane, such that fermions are strongly confined along the z direction and form a series of pancake-shaped clouds [27, 28]. Each such cloud can be considered as a quasi-2D Fermi gas when the axial confinement is strong enough to turn off inter-cloud tunnelling. The strong anisotropy of the trapping potentials, namely $\omega_z \gg \omega$ where $\omega_z(\omega)$ is the axial(radial) frequency, allows us to use an effective 2D Hamiltonian to deal with the radial degrees of freedom[28]. The effective binding energy $\epsilon_B = \hbar\omega_z \exp[4\pi a_z^2/U_p^{\text{eff}}(a_s, a_z)]$ is related to the energy scale $\hbar\omega_z$ and the 3D s-wave scattering length a_s , where a_z is defined as $a_z = \sqrt{\hbar/(m\omega_z)}$ and the quantity $U_p^{\text{eff}}(a_s, a_z)$ defined in [28] carries the dependence on 3D scattering length. By adjusting the 3D scattering length a_s and/or the axial frequency ω_z , a quasi-2D BCS-BEC crossover can be realized.

III. EQUATION OF STATE

We now turn on the Zeeman splitting $h \neq 0$. To determine the superfluid phase diagrams and calculate the density profile for imbalanced Fermi gas in a harmonic trap, we first establish the equations of state (EOS) for various phases in grand canonical ensemble[13]. In the BCS-Leggett mean field theory, the pressure $\mathcal{P} = -\Omega$ as a function of μ and h can be evaluated as[13]

$$\mathcal{P}(\mu, h) = c \int_0^\infty dz \left[E_z - z + \mu - \frac{\Delta^2}{2z + \epsilon_B} - (E_z - h)\Theta(h - E_z) \right] \quad (10)$$

with $E_z = \sqrt{(z - \mu)^2 + \Delta^2}$ and $c = M/(2\pi)$. We have set $h > 0$ without loss of generality. The superfluid order parameter $\Delta(\mu, h) = -U\langle\psi_\downarrow\psi_\uparrow\rangle$ is determined self-

consistently from the gap equation

$$\Delta \int_0^\infty dz \left[\frac{1}{2z + \epsilon_B} - \frac{\Theta(E_z - h)}{2E_z} \right] = 0. \quad (11)$$

The step function $\Theta(x)$ in this paper is defined as $\Theta(x) = 0$ for $x < 0$ and $\Theta(x) = 1$ for $x > 0$.

Unlike the 3D case[13], the EOS in 2D can be analytically obtained. At fixed μ and h , we have three possible phases: the unpolarized superfluid phase (SF), the polarized normal phase (N) and the polarized superfluid phase or Sarma phase (S) [2]. The phase SF corresponds to the solution $\Delta(\mu) = \sqrt{\epsilon_B(\epsilon_B + 2\mu)}$ in the region $h < E_g = \sqrt{\mu^2\Theta(-\mu) + \Delta^2(\mu)}$, and the pressure can be evaluated as

$$\mathcal{P}_{\text{SF}}(\mu) = c \left(\mu + \frac{\epsilon_B}{2} \right)^2 \quad (12)$$

which does not depend explicitly on h . The total number density $n = n_\uparrow + n_\downarrow$ and the magnetization $m = n_\uparrow - n_\downarrow$ can be expressed as

$$n_{\text{SF}}(\mu) = 2c \left(\mu + \frac{\epsilon_B}{2} \right), \quad m_{\text{SF}}(\mu) = 0. \quad (13)$$

The polarized superfluid phase or Sarma phase (S) corresponds to the solution in the region $h > E_g$. This phase can be ruled out from the positive secondary derivative [23]

$$\frac{\partial^2 \mathcal{P}}{\partial \Delta^2} \Big|_S = c \left[\frac{h(1 + \Theta(\mu))}{\sqrt{h^2 - \Delta^2}} - \frac{\mu\Theta(\mu)}{\sqrt{\mu^2 + \Delta^2}} - 1 \right] > 0, \quad (14)$$

which means that the Sarma phase is always unstable for any coupling in 2D.

The polarized normal phase corresponds to the solution $\Delta = 0$. The pressure takes the form of non-interacting Fermi gas,

$$\mathcal{P}_N(\mu, h) = \frac{c}{2} [(\mu - h)^2\Theta(\mu - h) + (\mu + h)^2\Theta(\mu + h)], \quad (15)$$

where the case $\mu + h < 0$ corresponds to the vacuum without atoms. For $\mu + h > 0$, the total number density and the magnetization read

$$\begin{aligned} n_N(\mu, h) &= 2c\mu\Theta(\mu - h) + c(\mu + h)\Theta(h - \mu), \\ m_N(\mu, h) &= 2ch\Theta(\mu - h) + c(\mu + h)\Theta(h - \mu). \end{aligned} \quad (16)$$

The cases $\mu > h$ and $\mu < h$ correspond to the partially polarized (N_{PP}) and fully polarized (N_{FP}) normal phases respectively. Since we treat the superfluid and normal phase in mean field approximation, the normal phase is considered as a non-interacting gas. In fully polarized case, this is correct since only s-wave interaction is considered. However, in partially polarized case, the interaction may be important in some coupling parameter region, like the finding around the unitary region in

3D [15, 16, 29]. Including fluctuations, which can not be treated analytically even in 2D, is necessary for a more realistic study.

Since the polarized superfluid phase is always located at the maximum of the thermodynamic potential, there exists at fixed μ a first order quantum phase transition from the SF phase to the normal phase when the Zeeman field h increases. The critical value h_c is determined by the condition $\mathcal{P}_{\text{SF}}(\mu) = \mathcal{P}_{\text{N}}(\mu, h_c)$. The analytical expression for h_c can be written as

$$h_c(\mu) = \sqrt{\epsilon_{\text{B}} \left(\mu + \frac{\epsilon_{\text{B}}}{4} \right)} \Theta(\mu - h_0) + \left[(\sqrt{2} - 1)\mu + \frac{\epsilon_{\text{B}}}{\sqrt{2}} \right] \Theta(h_0 - \mu). \quad (17)$$

Equivalently, for a given h , SF-N phase transition happens when the chemical potential μ becomes less than the critical value

$$\mu_c(h) = \left(\frac{h^2}{\epsilon_{\text{B}}} - \frac{\epsilon_{\text{B}}}{4} \right) \Theta(h - h_0) + \frac{\sqrt{2}h - \epsilon_{\text{B}}}{2 - \sqrt{2}} \Theta(h_0 - h), \quad (18)$$

where $h_0 = (\sqrt{2} + 1)\epsilon_{\text{B}}/2$ is determined by the equation $h_0 = \mu_c(h_0)$. We can easily prove that $h > h_0$ ($h < h_0$) is equivalent to the condition $\mu_c > h$ ($\mu_c < h$).

The grand canonical phase diagram in the $\mu - h$ plane is shown in Fig.1. The analytical expressions for the phase boundaries can be obtained from the above expression for h_c . The SF phase, N_{FP} phase and the vacuum meet at the point $(\mu, h) = (-\epsilon_{\text{B}}/2, \epsilon_{\text{B}}/2)$, while the three phases SF, N_{PP} and N_{FP} meet at $(\mu, h) = ((\sqrt{2} + 1)\epsilon_{\text{B}}/2, (\sqrt{2} + 1)\epsilon_{\text{B}}/2)$. The grand canonical phase diagram is of great help for us to understand the density profile in a harmonic trap.

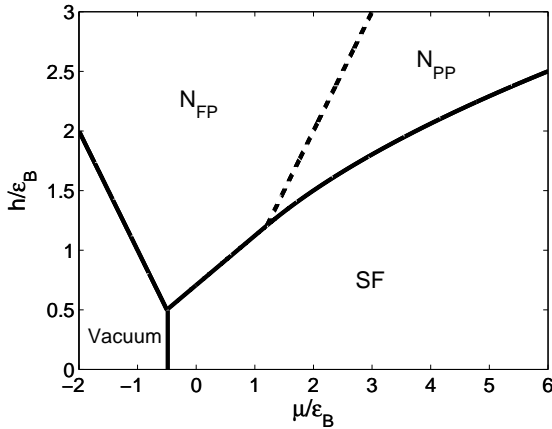


FIG. 1: The grand canonical phase diagram in the $\mu - h$ plane. μ and h are scaled by the binding energy ϵ_{B} .

IV. HOMOGENEOUS FERMION GAS

In this section we determine the phase diagram of the homogeneous system. Since the total atom number $N = N_{\uparrow} + N_{\downarrow}$ or equivalently the total atom density n is fixed, the chemical potential μ is not a free variable in the canonical ensemble and should be determined by the number conservation. One may distinguish two different cases: (1) The Zeeman field h can be experimentally adjusted by using Raman detuning[24]; (2) The atom number for each species, N_{\uparrow} and N_{\downarrow} , can be adjusted[4, 5]. Since the phase structure should be essentially independent of the ensemble we choose, we firstly discuss the phase diagram using h as tunable parameter, and then translate it into the case where the global polarization $P = (N_{\uparrow} - N_{\downarrow})/(N_{\uparrow} + N_{\downarrow})$ is directly adjusted.

A. Critical Zeeman Fields

We now consider the problem: When does the superfluidity disappear when a Zeeman splitting h is turned on? The total density n and the Zeeman field h are thermodynamic variables, and the free energy of the system should be defined as $\mathcal{F}(n, h) = \mu n - \mathcal{P}$. Since $n = M\epsilon_{\text{F}}/\pi$ is fixed, we will write $\mathcal{F}(n, h) = \mathcal{F}(h)$. At nonzero Zeeman field h , the solutions of the coupled gap and number equations corresponding to the above three homogeneous bulk phases can be analytically solved:

I. $\Delta_{\text{SF}}(h) = \Delta_0$ and $\mu_{\text{SF}}(h) = \mu_0$ in the phase SF. The solution exists in the region $0 < h < \Delta_0$ for $\eta < 2$ or $0 < h < \epsilon_{\text{F}} + \epsilon_{\text{B}}/2$ for $\eta > 2$.

II. $\Delta_{\text{N}}(h) = 0$ and $\mu_{\text{N}}(h) = \epsilon_{\text{F}}\Theta(\epsilon_{\text{F}} - h) + (2\epsilon_{\text{F}} - h)\Theta(h - \epsilon_{\text{F}})$ in the phase N. The first and second term correspond, respectively, to partially and fully polarized normal phase.

III. $\Delta_{\text{S}}(h) = \sqrt{\Delta_0(2h - \Delta_0)}$ and $\mu_{\text{S}}(h) = \epsilon_{\text{F}} - \Delta_{\text{S}}^2(h)/(4\epsilon_{\text{F}})$ in the region of $\Delta_0/2 < h < \Delta_0$ and $\eta < 2$ and $\Delta_{\text{S}}(h) = \sqrt{\epsilon_{\text{B}}(2h - \epsilon_{\text{B}})}$ and $\mu_{\text{S}}(h) = 2\epsilon_{\text{F}} - h$ in the region of $\epsilon_{\text{B}}/2 < h < \epsilon_{\text{F}} + \epsilon_{\text{B}}/2$ and $\eta > 2$ in the phase S. There are two gapless Fermi surfaces at $\eta < 2$ and only one gapless Fermi surface at $\eta > 2$.

The polarized superfluid phase or the Sarma phase, which is a gapless superfluid, is again an unstable state at any coupling, directly from the reentrance phenomenon (three solutions of Δ at fixed h), in contrast to the case in 3D where it becomes the stable ground state in the strong coupling BEC region [13, 14]. This is an important difference of the Fermi surface topology and the stability condition between 3D and 2D cases[23]. Explicitly, the free energy (density) $\mathcal{F}(h) = \mu(h)n - \mathcal{P}(\mu(h), h)$ in the three homogeneous bulk phases reads

$$\begin{aligned} \mathcal{F}_{\text{SF}}(h) &= c(\epsilon_{\text{F}}^2 - \epsilon_{\text{F}}\epsilon_{\text{B}}), \\ \mathcal{F}_{\text{N}}(h) &= c[(\epsilon_{\text{F}}^2 - h^2)\Theta(\epsilon_{\text{F}} - h) \\ &\quad + 2(\epsilon_{\text{F}}^2 - \epsilon_{\text{F}}h)\Theta(h - \epsilon_{\text{F}})], \\ \mathcal{F}_{\text{S}}(h) &= c[2(\epsilon_{\text{F}}^2 - \epsilon_{\text{F}}h) + h^2 + (h - \epsilon_{\text{B}}/2)^2]\Theta(\eta - 2) \end{aligned}$$

$$+ c[(\epsilon_F^2 - \epsilon_F \epsilon_B) + (\Delta_0 - h)^2] \Theta(2 - \eta). \quad (19)$$

It is easy to see that the polarized superfluid phase has always higher free energy. If there exist no other possible phases, a first order quantum phase transition from the phase SF to the phase N will occur at a critical Zeeman field h_c determined by $\mathcal{F}_{\text{SF}}(h_c) = \mathcal{F}_{\text{N}}(h_c)$. We find $h_c = \sqrt{\eta} \epsilon_F = \Delta_0 / \sqrt{2}$ for $\eta < 1$ and $h_c = \frac{1}{2}(1 + \eta) \epsilon_F$ for $\eta > 1$. It is interesting to note that the relation $h_c = \Delta_0 / \sqrt{2}$ at $\eta < 1$ is only an approximate result at weak coupling in 3D [1, 2].

If there are only the two bulk phases SF and N, we have only one CC limit at which the first order phase transition occurs, and the experimentally observed phase separation (PS) will be hidden in the η - h phase diagram. However, since the total atom density n is fixed, unlike the grand canonical ensemble, we should consider possible mixed phases constructed via the Gibbs phase equilibrium condition. Here we will neglect the interfacial energy [30], since for a macroscopic phase separation, this energy contribution is subdominant in the thermodynamic limit. From equation (14), the only possibility is the SF-N mixed phase. When the phase separation is favored in a region $h_{c1} < h < h_{c2}$, the chemical potential μ_{PS} is different from μ_{SF} and μ_{N} , it should be determined by the phase equilibrium condition $\mathcal{P}_{\text{SF}}(\mu) = \mathcal{P}_{\text{N}}(\mu, h)$, which leads to

$$\begin{aligned} \mu_{\text{PS}}(h) &= \left(\frac{h^2}{\epsilon_B} - \frac{\epsilon_B}{4} \right) \Theta(h - h_0) \\ &+ \frac{\sqrt{2}h - \epsilon_B}{2 - \sqrt{2}} \Theta(h_0 - h), \end{aligned} \quad (20)$$

where $h_0 = (\sqrt{2} + 1)\epsilon_B/2$ satisfies the equation $h_0 = \mu_{\text{PS}}(h_0)$. Since the chemical potential μ_{PS} is determined by the condition $\mathcal{P}_{\text{SF}}(\mu) = \mathcal{P}_{\text{N}}(\mu, h)$, it is equivalent to the critical chemical potential $\mu_c(h)$ in the grand canonical ensemble. The cases $h > h_0$ and $h < h_0$ indicate, respectively, the mixed phases with partially polarized normal bubbles (SF-N_{PP}) and fully polarized normal bubbles (SF-N_{FP}). The volume fractions of the phases SF and N in the phase separation, denoted by x and $1 - x$ respectively, are determined by the number conservation, $n = x(h)n_{\text{SF}}(\mu_{\text{PS}}, h) + [1 - x(h)]n_{\text{N}}(\mu_{\text{PS}}, h)$. Using the expressions (13), (16) and (20) for μ_{PS} , n_{N} and n_{SF} , we find

$$\begin{aligned} x(h) &= 2 \left(\frac{\epsilon_F}{\epsilon_B} + \frac{1}{4} - \frac{h^2}{\epsilon_B^2} \right) \Theta(h - h_0) \\ &+ \left(\frac{2\sqrt{2}\epsilon_F}{2h - \epsilon_B} - \sqrt{2} - 1 \right) \Theta(h_0 - h). \end{aligned} \quad (21)$$

We now determine the region of the mixed phase, i.e., the lower and upper critical fields h_{c1} and h_{c2} [13]. In the grand canonical ensemble with fixed chemical potential μ , we have only one critical field $h_c(\mu)$ determined by the condition $\mathcal{P}_{\text{SF}}(\mu, h) = \mathcal{P}_{\text{N}}(\mu, h)$, and the signal of SF-N phase separation is denoted by the first order

phase transition line in the μ - h phase diagram. In the standard BCS-BEC crossover problem, the total atom number N rather than the chemical potential μ is fixed, and the CC limit splits into two values $h_{c1} = h_c(\mu_{\text{SF}})$ and $h_{c2} = h_c(\mu_{\text{N}})$ [13]. The mixed phase links continuously the phases SF and N with $\mu_{\text{PS}} = \mu_{\text{SF}}$ at $h = h_{c1}$ and $\mu_{\text{PS}} = \mu_{\text{N}}$ at $h = h_{c2}$ and ensures $0 \leq x \leq 1$ with $x(h_{c1}) = 1$ and $x(h_{c2}) = 0$. The critical fields h_{c1} and h_{c2} are explicitly given by

$$\begin{aligned} h_{c1} &= \epsilon_F \sqrt{\eta \left(1 - \frac{\eta}{4} \right)} \Theta(\eta_1 - \eta), \\ &+ \epsilon_F \left(\sqrt{2} - 1 + \frac{\eta}{2} \right) \Theta(\eta - \eta_1), \\ h_{c2} &= \epsilon_F \sqrt{\eta \left(1 + \frac{\eta}{4} \right)} \Theta(\eta_2 - \eta), \\ &+ \epsilon_F \left(2 - \sqrt{2} + \frac{\eta}{2} \right) \Theta(\eta - \eta_2), \end{aligned} \quad (22)$$

where $\eta_1 = 2 - \sqrt{2} \simeq 0.586$ and $\eta_2 = 2(\sqrt{2} - 1) \simeq 0.828$ are determined by $\mu_{\text{SF}}(h_0) = h_0$ and $\mu_{\text{N}}(h_0) = h_0$, respectively. There is always the relation $h_{c1} < h_c < h_{c2}$, and the splitting disappears in the weak coupling limit $\eta \rightarrow 0$ which recovers the well known result shown in [1, 2]. On the other hand, the splitting keeps as a constant $(3 - 2\sqrt{2})\epsilon_F \simeq 0.172\epsilon_F$ at strong coupling $\eta > \eta_2$.

The final step is to prove that the SF-N mixed phase has the lowest free energy in the region $h_{c1} < h < h_{c2}$. Using the analytical expressions for $x(h)$ and $\mu_{\text{PS}}(h)$ as well as the EOS for the phases SF and N, we can evaluate the free energy in the mixed phase defined by $\mathcal{F}_{\text{PS}}(h) = \mu_{\text{PS}} n - x(h)\mathcal{P}_{\text{SF}}(\mu_{\text{PS}}, h) - [1 - x(h)]\mathcal{P}_{\text{N}}(\mu_{\text{PS}}, h)$. The difference between \mathcal{F}_{PS} and \mathcal{F}_{SF} and between \mathcal{F}_{PS} and \mathcal{F}_{N} can be explicitly expressed as

$$\begin{aligned} \mathcal{F}_{\text{PS}}(h) - \mathcal{F}_{\text{SF}}(h) &= -\epsilon_B^{-2} c(h^2 - h_{c1}^2)^2 \Theta(h - h_0) \\ &- (\sqrt{2} + 1)^2 c(h - h_{c1})^2 \Theta(h_0 - h), \\ \mathcal{F}_{\text{PS}}(h) - \mathcal{F}_{\text{N}}(h) &= -\epsilon_B^{-2} c(h^2 - h_{c2}^2)^2 \Theta(h - h_0) \\ &- (\sqrt{2} + 1)^2 c(h - h_{c2})^2 \Theta(h_0 - h). \end{aligned} \quad (23)$$

The above expressions show explicitly that the mixed phase has really the lowest free energy in the region $h_{c1} < h < h_{c2}$. While in 3D the conclusion that the mixed phase corresponds to the lowest free energy is analytically proven in the weak coupling limit [10], our result here in 2D is for any coupling.

The SF-N mixed phase has a nonzero global polarization P since the normal bubble is polarized. From the definition $P = (N_{\uparrow} - N_{\downarrow}) / (N_{\uparrow} + N_{\downarrow})$ we find

$$P(h) = [1 - x(h)] \frac{m_{\text{N}}(\mu_{\text{PS}}, h)}{n}. \quad (24)$$

Using the expression for $x(h)$ and μ_{PS} , we have

$$\begin{aligned} P(h) &= \frac{2h(h^2 - h_{c1}^2)}{\epsilon_F \epsilon_B^2} \Theta(h - h_0) \\ &+ \frac{(\sqrt{2} + 1)^2 (h - h_{c1})}{\epsilon_F} \Theta(h_0 - h). \end{aligned} \quad (25)$$

The global polarization is zero at $h = h_{c1}$ and then increases with h .

B. Critical Polarization

Finally, we convert the above result into the one where both N_\uparrow and N_\downarrow are fixed and the exchange between particles in states \uparrow and \downarrow is forbidden, corresponding to recent experiments on ultracold Fermi gas with population imbalance[4, 5]. The free energy density in this case should be defined as $\mathcal{F}(n_\uparrow, n_\downarrow) = \mu_\uparrow n_\uparrow + \mu_\downarrow n_\downarrow - \mathcal{P}$ or $\mathcal{F}(n, m) = \mu n + m h - \mathcal{P}$. The possible phases with nonzero global polarization P are the normal, Sarma and SF-N mixed phases. Since the phase structure should be essentially independent of the ensemble we choose[13], we do not need to compare again the free energies of the three phases[10]. Since $P(h_{c1}) = 0$ and $P(h)$ increases with h , we conclude that the ground state is the unpolarized superfluid at $P = 0$, and SF-N phase separation becomes energetically favored for $0 < P < P_c$. The critical polarization P_c where the superfluid bubble disappears completely is the global polarization at h_{c2} ,

$$\begin{aligned} P_c &= P(h_{c2}) = \frac{h_{c2}}{\epsilon_F} \Theta(\eta_2 - \eta) + \Theta(\eta - \eta_2) \\ &= \sqrt{\eta(1 + \frac{\eta}{4})} \Theta(\eta_2 - \eta) + \Theta(\eta - \eta_2). \end{aligned} \quad (26)$$

The critical polarization increases from $P_c = 0$ at $\eta = 0$ to $P_c = 1$ at $\eta = \eta_2$ and then keeps as a constant $P_c = 1$ at strong coupling $\eta > \eta_2$

C. Phase Diagrams

Fig.2 summarizes the above analytical results. The phase diagram in the $\eta - h$ plane is shown in the upper panel. The partially and fully polarized normal phases N_{PP} and N_{FP} are separated by the dashed line $h/\epsilon_F = 1$ which ends at $\eta = \eta_2$. The two solid lines indicate the lower and upper critical Zeeman fields h_{c1} and h_{c2} with the two phase separations PS-I and PS-II in between. PS-I (SF- N_{PP}) and PS-II (SF- N_{FP}) are the mixed phases of superfluid and normal gas with N_{PP} and N_{FP} , and they are separated by the dotted line $h/\epsilon_F = (\sqrt{2} + 1)\eta/2$ starting at $\eta = \eta_1$ and ending at $\eta = \eta_2$. The phase diagram in the $\eta - P$ plane can be easily converted into the one in the $\eta - P$ plane shown in the lower panel, by taking the fact $P(h_{c1}) = 0$ and $P(h_{c2}) = P_c$. The critical polarization $P_c = \sqrt{\eta(1 + \eta/4)}$ (solid line) increases from $P_c = 0$ at $\eta = 0$ to $P_c = 1$ at $\eta = \eta_2$ and then keeps as a constant $P_c = 1$ for $\eta > \eta_2$. The phases SF and N_{FP} are now located at $P = 0$ and $P = 1$ respectively. The dotted line which separates PS-I from PS-II becomes $P = (4 + 3\sqrt{2})\eta/2 - (\sqrt{2} + 1)$ in the $\eta - P$ plane.

The above analytical results show that, to correctly calculate the critical polarization P_c and the phase diagrams, one should treat the mixed phase carefully [13].

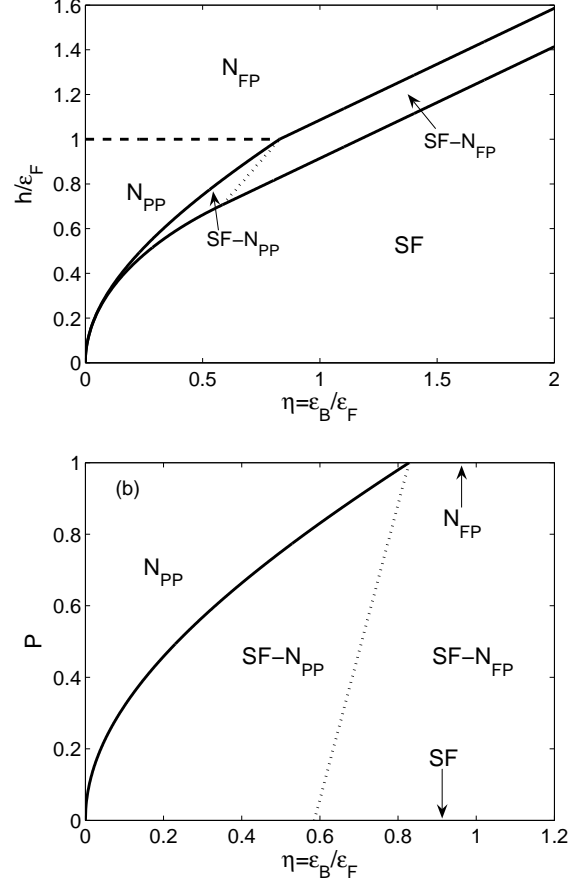


FIG. 2: The phase diagrams in the planes $\eta - h$ (upper panel) and $\eta - P$ (lower panel). h is scaled by the Fermi energy. SF means unpolarized superfluid, N_{PP} and N_{FP} indicate the partially and fully polarized normal phases, and SF- N_{PP} and SF- N_{FP} are the mixed phases of superfluid and normal gas with N_{PP} and N_{FP} .

Some other methods taken in literatures may lead to quantitatively incorrect results. For instance, the method of stability analysis will result in an incorrect critical polarization (see also the comments in [32]). With this method, one first solve the mean field gap and number equations for the Sarma phase and then analyze the stability of this phase. If it is applied to the 2D system, the critical polarization becomes [31]

$$P_c = \frac{\Delta_0}{2\epsilon_F} = \sqrt{\frac{\eta}{2}}, \quad (27)$$

which is the maximum polarization of the unstable Sarma phase and deviates significantly from our result $P_c = \sqrt{\eta(1 + \eta/4)}$. Especially, our critical polarization grows up to unity at $\eta \simeq 0.828$, but the result (27) becomes unity at $\eta = 2$. On the other hand, if one takes only the phases SF and N into account but neglect the phase separation, there will be only one critical field h_c where the polarization jumps from 0 to $h_c/\epsilon_F = \sqrt{\eta}$.

V. BOUND STATE IN POLARIZED NORMAL PHASE

In recent experiment on highly polarized normal phase in 3D unitary Fermi gas[8], it is found that while the superfluidity disappears completely, full pairing of minority atoms always exists, which indicates that the fermion pairing may be easy to occur in the presence of polarization. It is well known that the bound state in 2D can form at arbitrary small attractive interaction[26], which is quite different to the 3D case. It is natural to ask: Do the di-fermion bound states exist above the upper critical field h_{c2} or critical polarization P_c ?

In this section, we study the spectrum of bound states in the highly polarized normal phase. In the Green function method, the energy ω of the bound states with zero total momentum in this case is determined through the equation [22]

$$\int_0^\infty dz \left[\frac{1}{2z + \epsilon_B} - \frac{1 - \Theta(\mu_\uparrow - z) - \Theta(\mu_\downarrow - z)}{2z - 2\mu - \omega} \right] = 0. \quad (28)$$

In the vacuum with $\mu = h = 0$, it self-consistently gives the solution $\omega = -\epsilon_B$. In general case with medium effect, the bound states can survive when the above equation has real solution of ω .

The integration in the above equation can be analytically worked out, and finally we obtain

$$\ln \frac{\omega + 2\mu}{-\epsilon_B} + \Theta(\mu - h) \ln \frac{\omega + 2h}{\omega + 2\mu} + \Theta(\mu + h) \ln \frac{\omega - 2h}{\omega + 2\mu} = 0. \quad (29)$$

In the partially polarized normal phase, we have $\mu = \epsilon_F$, the spectrum equation becomes

$$\omega^2 + \epsilon_B \omega + 2\epsilon_F \epsilon_B - 4h^2 = 0 \quad (30)$$

which has real solutions

$$\omega = -\frac{1}{2} \left(\epsilon_B \pm \sqrt{J(h)} \right) \quad (31)$$

for

$$J(h) = \epsilon_B^2 + 16h^2 - 8\epsilon_B \epsilon_F > 0. \quad (32)$$

In the fully polarized normal phase, one finds that the spectrum equation directly gives a real solution $\omega = 2h - \epsilon_B$. However, this solution is unphysical since we always have $\omega > 0$. This can be well understood when we consider the fact that there exist only \uparrow particles in this phase.

In the balanced normal phase with $h = 0$ (note that the true ground state in this case is the superfluid phase), the bound states remain stable only at strong enough coupling $\eta > 8$ or equivalently low enough density $\epsilon_F < \epsilon_B/8$ [22], which indicates that the Fermi sea or medium effect disfavors the formation of bound states. One may simply think that, the presence of a Zeeman splitting will further destroy the bound states. However, this is

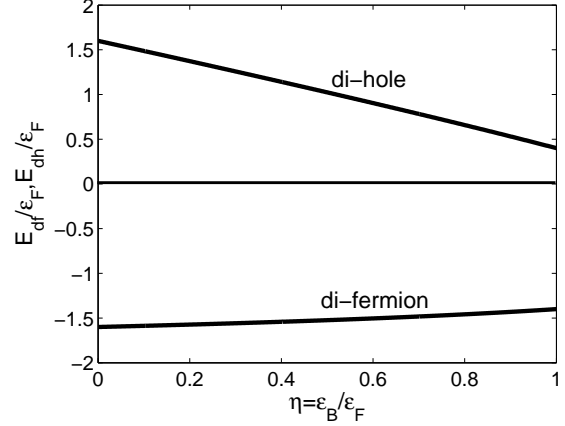


FIG. 3: The excitation gaps for the di-fermions and di-holes as a function of η at fixed polarization $P = 0.8$. The curves are meaningful only for $\eta < 0.56$, since the ground state is not a normal phase for $\eta > 0.56$.

not true. Since the condition $J(h) > 0$ is easier to be satisfied at $h \neq 0$, the bound states in highly polarized normal phase are easier to survive than in the balanced Fermi sea. In the whole partially polarized normal phase which exists in the region $0 < \eta < \eta_2$ in Fig.2, we have $\epsilon_F \sqrt{\eta(1 - \eta/4)} < h < \epsilon_F$. Analyzing the condition $J(h) > 0$, we conclude the bound states can exist in the whole N_{PP} phase in Fig.2. Especially, they can survive at high polarization even in the weak coupling limit, as pointed out in [33] in the case of 3D.

There exist two real solutions for ω in the N_{PP} phase. The negative ($\omega < 0$) and positive ($\omega > 0$) solutions in (31) correspond to the excitation gaps E_{df} and E_{dh} for the di-fermions(df) and di-holes(dh) respectively[33],

$$\begin{aligned} E_{df} &= -\frac{\epsilon_F}{2} \left(\eta + \sqrt{\eta^2 - 8\eta + 16P^2} \right), \\ E_{dh} &= \frac{\epsilon_F}{2} \left(\sqrt{\eta^2 - 8\eta + 16P^2} - \eta \right). \end{aligned} \quad (33)$$

In Fig.3, we plot the excitation gaps for di-fermions and di-holes at a fixed polarization $P = 0.8$. We found that the symmetry in the spectrum ($E_{df} = -E_{dh}$) holds only at weak coupling.

VI. DENSITY PROFILE IN A HARMONIC TRAP

We have determined the phase diagram for homogeneous system. However, the phase structure can not be directly examined in ultracold Fermi gas experiments, due to the effect of the external harmonic trap. To justify the theoretical prediction for homogeneous system, one should calculate the corresponding phase diagram and the density profile in the presence of an external trap potential, using the same equation of state. In this

section, we will calculate analytically the density profile of an imbalance Fermi gas in a 2D isotropic harmonic trap potential $V(r) = \frac{1}{2}M\omega^2 r^2$. The frequency ω here is different from the energy of the bound state defined in Section V.

The effect of a harmonic trap can be treated in the local density approximation(LDA). In the frame of LDA, the system is approximately taken to be uniform but with a local chemical potential given by

$$\mu(r) = \mu_0 - \frac{1}{2}M\omega^2 r^2, \quad (34)$$

where μ_0 is the chemical potential at the center of the trap and is the true chemical potential(a Lagrangian multiplier) still enforcing the total atom number $N = N_\uparrow + N_\downarrow$. Since N_\uparrow and N_\downarrow are both conserved, the spatially-varying spin-up and spin-down local chemical potentials can be expressed as $\mu_\uparrow(r) = \mu(r) + h$ and $\mu_\downarrow(r) = \mu(r) - h$ in terms of the averaged chemical potential $\mu(r)$ and Zeeman field h .

To calculate the density profile, namely the atom density of the spin-up and spin-down states as a function of the radius r , $n_\uparrow(r)$ and $n_\downarrow(r)$, or equivalently the total density $n(r) = n_\uparrow(r) + n_\downarrow(r)$ and the magnetization $m(r) = n_\uparrow(r) - n_\downarrow(r)$, one should know the equation of state, $n_\sigma(r) = n_\sigma(\mu(r), h)$ with $\sigma = \uparrow, \downarrow$. Using the EOS calculated in Section III, we can determine μ_0 and h from the known total particle number N and the global polarization $P = (N_\uparrow - N_\downarrow)/(N_\uparrow + N_\downarrow)$,

$$N = 2\pi \int r dr n(r), \quad PN = 2\pi \int r dr m(r). \quad (35)$$

Let us firstly consider a non-interacting system with balanced populations, $N_\uparrow = N_\downarrow$, which can help us to define the Fermi energy ϵ_F for trapped 2D system. ϵ_F is defined as the chemical potential μ_0 at the center of the trap for non-interacting gas. The density profile is also balanced, $n_\uparrow(r) = n_\downarrow(r)$, and is given by

$$n_\uparrow(r) = n_\downarrow(r) = c \left(\epsilon_F - \frac{1}{2}M\omega^2 r^2 \right), \quad (36)$$

which vanishes at the so called Thomas-Fermi radius

$$R_T = \sqrt{\frac{2\epsilon_F}{M\omega^2}}. \quad (37)$$

The total density N is then given by the integral

$$N = 2\pi \int_0^{R_T} r dr 2c \left(\epsilon_F - \frac{1}{2}M\omega^2 r^2 \right) = \left(\frac{\epsilon_F}{\hbar\omega} \right)^2. \quad (38)$$

We find that the Fermi energy in 2D is $\epsilon_F = \sqrt{N}\hbar\omega$, in contrast to the result $\epsilon_F = (6N)^{1/3}\hbar\omega$ in 3D (note that we have recovered \hbar in these expressions).

We then turn to an attractive Fermi gas. For balanced populations, the ground state is a superfluid state, and the density profile can be obtained from equation (13),

$$n_\uparrow(r) = n_\downarrow(r) = c \left(\mu_0 + \frac{\epsilon_B}{2} - \frac{1}{2}M\omega^2 r^2 \right). \quad (39)$$

Comparing with the non-interacting gas, we find no difference between the normal and the superfluid states. The chemical potential at the center of the trap reads

$$\mu_0 = \sqrt{N}\hbar\omega - \frac{\epsilon_B}{2} = \epsilon_F - \frac{\epsilon_B}{2}. \quad (40)$$

This relation is exactly the same as in the homogeneous case[19]. The order parameter profile $\Delta(r)$ is given by

$$\Delta(r) = \Delta_0 \sqrt{1 - r^2/R_T^2}, \quad \Delta_0 = \sqrt{2\epsilon_B\epsilon_F}. \quad (41)$$

For a system with population imbalance, $N_\uparrow \neq N_\downarrow$, we should have $h \neq 0$. By comparing \mathcal{P}_{SF} with \mathcal{P}_N , a first order phase transition from the phase SF to the phase N occurs for a given μ when the Zeeman field h becomes larger than the critical value $h_c(\mu)$, or equivalently speaking, for a given h the SF-N phase transition happens when the chemical potential μ becomes less than the critical value $\mu_c(h)$. In LDA, the phase behavior as a function of chemical potential μ is translated into a spatial cloud profile through $\mu(r)$. The critical phase boundary μ_c corresponding to the critical radius r_c is defined by

$$\mu_c = \mu(r_c) = \mu_0 - \frac{1}{2}M\omega^2 r_c^2 \quad (42)$$

at which the states SF and N have the same pressure. Thus, at fixed h , any region of the system which satisfies $\mu(r) > \mu_c$ is in the state SF, while a region which satisfies $\mu(r) < \mu_c$ will be in the state N. Since $\mu(r)$ decreases with increasing r , it is clear that the high density superfluid region will be confined in the center of the trap, and the low density polarized state N is expelled to the outside. The shell structure with radius r_c of the SF-N interface is a striking signature of phase separation in a trap. The superfluid core will disappear when the population imbalance P becomes larger than the critical value P_c which is determined by the equation $r_c = 0^+$ or $\mu_0 = \mu_c$.

We should have two types of shell structure corresponding to the cases $h > h_0$ and $h < h_0$. For the case $h > h_0$, we have $\mu(r_c) = \mu_c = h^2/\epsilon_B - \epsilon_B/4 > h$, which means that there exists a shell of partially polarized normal gas in the region $r_c < r < r_0$, with r_0 given by $\mu(r_0) = h$. We call it the phase PS-I. Thus we have the following density profile

$$n(r) = \begin{cases} 2c \left(\mu_0 + \frac{\epsilon_B}{2} - \frac{1}{2}M\omega^2 r^2 \right) & , \quad 0 < r < r_c \\ 2c \left(\mu_0 - \frac{1}{2}M\omega^2 r^2 \right) & , \quad r_c < r < r_0 \\ c \left(\mu_0 + h - \frac{1}{2}M\omega^2 r^2 \right) & , \quad r_0 < r < R \end{cases} \quad (43)$$

and

$$m(r) = \begin{cases} 0 & , \quad 0 < r < r_c \\ 2ch & , \quad r_c < r < r_0 \\ c \left(\mu_0 + h - \frac{1}{2}M\omega^2 r^2 \right) & , \quad r_0 < r < R \end{cases} \quad (44)$$

where $R = \sqrt{2(\mu_0 + h)/M\omega^2}$ is the edge of the cloud. After some algebra according to the equation (35), μ_0 is

simply given by $\mu_0 = \epsilon_F - \epsilon_B/2$ as in the balanced case and h is solved from the cubic equation

$$2h \left(\frac{h^2}{\epsilon_B} - \frac{\epsilon_B}{4} \right) = P\epsilon_F^2, \quad (45)$$

where $\epsilon_F = \sqrt{N}\hbar\omega$ is the Fermi energy defined in (38).

From the condition $h > h_0$ which ensures $r_0 > r_c$, we have $P\epsilon_F^2 > 2h_0^2$, which leads to the relation

$$P > P_0 = \frac{3 + 2\sqrt{2}}{2}\eta^2. \quad (46)$$

The critical polarization P_c is determined by the condition $\mu_0 = \mu_c$. A simple algebra gives

$$P_c = (2 - \eta)\sqrt{\eta - \frac{\eta^2}{4}}, \quad 0 < \eta < \eta_1 \quad (47)$$

with $\eta_1 = 2 - \sqrt{2} \simeq 0.586$. Note that both P_0 and P_c reach unity at $\eta = \eta_1$, they are the two boundaries of the phase PS-I in the $\eta - P$ plane.

For the case $h < h_0$ or $P < P_0$, we have $\mu(r_c) = \mu_c = (\sqrt{2}h - \epsilon_B)/(2 - \sqrt{2}) < h$, which means that the normal gas shell outside the superfluid core is fully polarized. The density profile reads

$$n(r) = \begin{cases} 2c(\mu_0 + \frac{\epsilon_B}{2} - \frac{1}{2}M\omega^2 r^2) & , \quad 0 < r < r_c \\ c(\mu_0 + h - \frac{1}{2}M\omega^2 r^2) & , \quad r_c < r < R \end{cases} \quad (48)$$

and

$$m(r) = \begin{cases} 0 & , \quad 0 < r < r_c \\ c(\mu_0 + h - \frac{1}{2}M\omega^2 r^2) & , \quad r_c < r < R \end{cases} \quad (49)$$

After the integration in equation (35), we still have $\mu_0 = \epsilon_F - \epsilon_B/2$ and h is explicitly given by

$$h = (\sqrt{2} - 1)\sqrt{P}\epsilon_F + \frac{\epsilon_B}{2}. \quad (50)$$

One can easily check that the condition $h < h_0$ is equivalent to $P > P_0$, and we have $P_c = 1$ for $\eta > \eta_1$.

Fig.4 summarizes the coupling-imbalance phase diagram for two-dimensional imbalanced Fermi gas in a harmonic trap. The critical polarization $P_c = (2 - \eta)\sqrt{\eta - \eta^2/4}$ (solid line) increases from $P_c = 0$ at $\eta = 0$ to $P_c = 1$ at $\eta = \eta_1 \simeq 0.586$ and then keeps as a constant $P_c = 1$ for $\eta > \eta_1$. The dashed line, analytically given by $P = (3 + 2\sqrt{2})\eta^2/2$, separates the two types of phase separation, PS-I and PS-II with different shell structure. In the phase PS-I, the density profile exhibits a SF-N_{PP}-N_{FP} shell structure, while in the phase PS-II, the shell is in the form of SF-N_{FP}.

The analytical result of the density profile can be summarized as follows. In the region PS-I, we have

$$\frac{n(r)}{n_0} = \begin{cases} 2(1 - x^2) & , \quad 0 < x < x_c \\ 2(1 - \frac{\eta}{2} - x^2) & , \quad x_c < x < x_0 \\ 1 - \frac{\eta}{2} + \delta - x^2 & , \quad x_0 < x < X \end{cases} \quad (51)$$

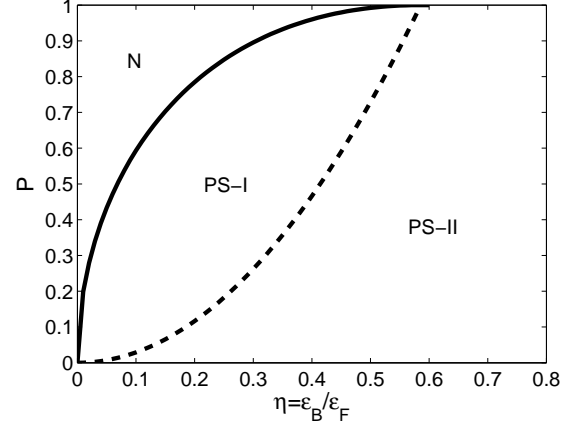


FIG. 4: Global phase diagram for trapped 2D Fermi gas in the $\eta - P$ plane.

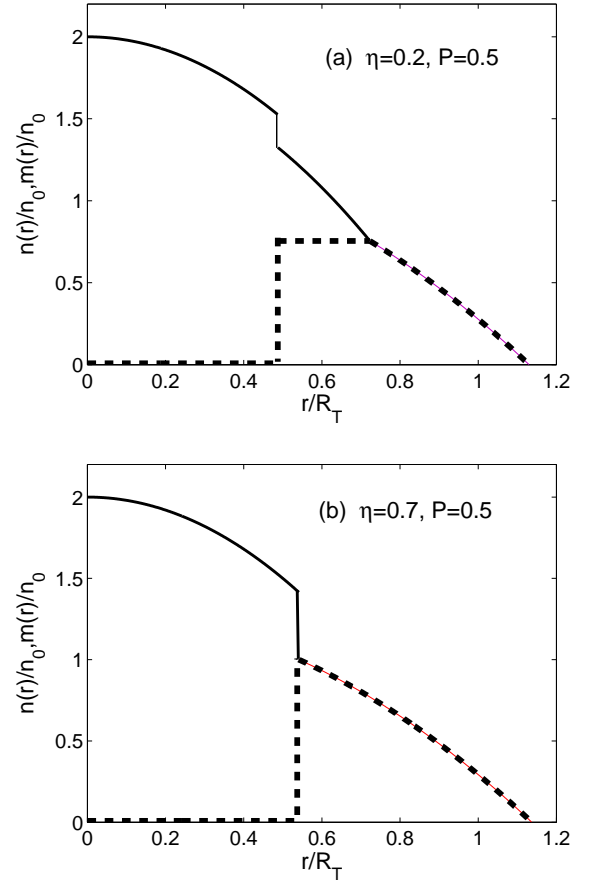


FIG. 5: The profiles for the total density $n(r)$ (solid line) and magnetization $m(r)$ (dashed line) in two cases, $\eta = 0.2$ and $P = 0.5$ in the region PS-I and $\eta = 0.7$ and $P = 0.5$ in the region PS-II.

and

$$\frac{m(r)}{n_0} = \begin{cases} 0 & , \quad 0 < x < x_c \\ 2\delta & , \quad x_c < x < x_0 \\ 1 - \frac{\eta}{2} + \delta - x^2 & , \quad x_0 < x < X \end{cases} \quad (52)$$

with $n_0 = c\epsilon_F$, $x = r/R_T$, R_T being the Thomas-Fermi radius of non-interacting gas defined in (37), and $\delta = h/\epsilon_F$ being the real solution of the cubic equation $\delta^3 - \eta^2\delta/4 - P\eta/2 = 0$,

$$\delta = \left(\frac{P\eta}{4}\right)^{1/3} \left[(1+\gamma)^{1/3} + (1-\gamma)^{1/3}\right] \quad (53)$$

with $\gamma = \sqrt{1 - \eta^4/(108P^2)}$. The scaled radii $x_c = r_c/R_T$, $x_0 = r_0/R_T$ and $X = R/R_T$ are given by

$$\begin{aligned} x_c &= \sqrt{1 - \frac{\eta}{2} - \frac{P}{2\delta}}, \\ x_0 &= \sqrt{1 - \frac{\eta}{2} - \delta}, \\ X &= \sqrt{1 - \frac{\eta}{2} + \delta}. \end{aligned} \quad (54)$$

A numerical sample for $\eta = 0.2, P = 0.5$ is shown in Fig.5(a). There is an interesting phenomenon which is different from that found in 3D: The magnetization profile $m(r)$ exhibits a visible platform structure in the partially polarized normal shell in the region $r_c < r < r_0$. For partially polarized gas, the interaction may be important, like the finding around the unitary region in 3D [15, 16, 29]. However, for the 2D system, since partially polarized normal shell appears only at small coupling where the effect of interaction is not important, our conclusion will not be qualitatively changed. We also observe a density jump Δn at the critical radius r_c . In the region PS-I, Δn is independent of the global polarization and depends only on the coupling strength,

$$\Delta n = \eta n_0 = \frac{M}{2\pi} \epsilon_B. \quad (55)$$

Thus the experimental data for Δn can be used to extract the effective two-body binding energy ϵ_B .

In the region PS-II, the density profile reads

$$\frac{n(r)}{n_0} = \begin{cases} 2(1-x^2) & , \quad 0 < x < x_c \\ 1 + (\sqrt{2}-1)\sqrt{P} - x^2 & , \quad x_c < x < X \end{cases} \quad (56)$$

and

$$\frac{m(r)}{n_0} = \begin{cases} 0 & , \quad 0 < x < x_c \\ 1 + (\sqrt{2}-1)\sqrt{P} - x^2 & , \quad x_c < x < X \end{cases} \quad (57)$$

The scaled radii x_c and X now takes very simple form

$$\begin{aligned} x_c &= \sqrt{1 - \sqrt{P}}, \\ X &= \sqrt{1 + (\sqrt{2}-1)\sqrt{P}}. \end{aligned} \quad (58)$$

A numerical sample of the density profile for $\eta = 0.7, P = 0.5$ is shown in Fig.5(b). It is very surprising that the density profile does not depend on the coupling parameter η , but only on the global polarization P . As a result, the ratio r_c/R exhibits a universal behavior when $\eta > \eta_1 = 0.586$, as shown in Fig.6.

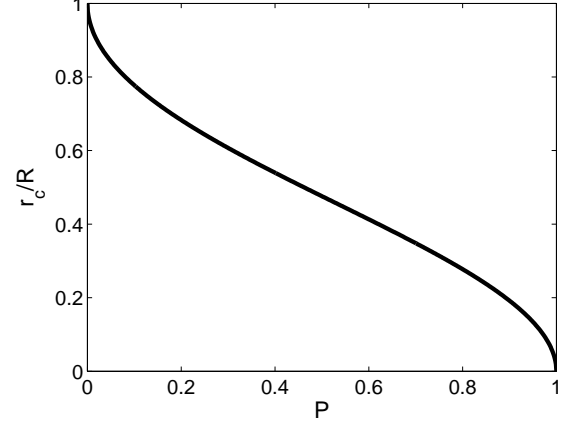


FIG. 6: The ratio of the superfluid radius to the cloud radius as a function of the global polarization P for $\eta > \eta_1 = 0.586$.

Finally, two comments on our results should be made. The first is on the BCS-Leggett mean field theory. In this theory, the quantum fluctuation in the superfluid phase and the interaction in the partially polarized phase are totally neglected. The effect of interaction in the partially polarized phase may change the platform structure in the region $r_c < r < r_0$. However, since the three-shell structure appears in the weak coupling region, we expect this effect to be small. At very strong coupling, the correction in the superfluid phase due to quantum fluctuation should be important, and the universal behavior in the region PS-II may be destroyed. Since the BEC region is reached at $\eta > 2$, we expect that our conclusion holds at the BCS side $\eta_1 < \eta < 2$. The second comment is on the model we used. Recently, it is argued that the model we used is not sufficient to discuss BCS-BEC crossover in quasi-2D Fermi gas due to the importance of dressed molecules[28]. However, from the study in [28], this effect is important only at strong coupling (may be for $\eta > 2$). Obviously, the comparison of our prediction with the experimental data can tell us whether the quantum fluctuation, dressed molecules and other possible effects are important.

VII. SUMMARY

In summary, mean field phase structure of polarized Fermi gas in 2D is analytically investigated. In the normal phase, the di-fermion bound states at high polarization are easier to survive than in the balanced Fermi

sea. In the BCS-Leggett mean field theory, the transition from the unpolarized superfluid phase to the normal phase is always of first order, and there exists no stable gapless superfluid phase. In the homogeneous system, we analytically determined the critical Zeeman fields and the critical population imbalance in the whole coupling parameter region. We found two critical Zeeman fields in the BCS-BEC crossover, and proved that the mixed superfluid-normal phase is the energetically favored ground state. However, from recent Monte-Carlo simulations [15, 16], our mean field results may be only qualitatively correct in some parameter region, due to the importance of interactions in the normal phase.

To compare our theoretical results with future experimental data, we have also calculated analytically the density profile for an imbalanced 2D Fermi gas confined in a harmonic trap. For balanced populations, the den-

sity profiles for normal and superfluid matter are the same and can not be used as a signature of superfluidity. For imbalanced populations, the density profile exhibits a shell structure, a superfluid core in the center and a normal shell outside. At small coupling, there exists a partially polarized normal shell and the density difference shows a platform structure. For large attraction, however, the normal shell is fully polarized, and the density profile depends only on the global population imbalance. Our theoretical prediction can be examined in the future experiments on 2D ultracold Fermi gases, which can help us to see whether quantum fluctuations and other possible effects are important in determining the phase structure[28].

Acknowledgments: The work is supported by the NSFC Grants 10575058 and 10735040 and the National Research Program Grant No.2006CB921404.

-
- [1] B.S.Chandrasekhar, Appl. Phys. Lett.**1**,7(1962); A.M.Clogston, Phys. Rev. Lett.**9**, 266(1962)
 - [2] G.Sarma, J. Phys. Chem. Solid **24**,1029(1963)
 - [3] P.Fulde and R.A.Ferrell, Phys. Rev. **A135**, 550(1964); A.I.Larkin and Yu.N.Ovchinnikov, Sov. Phys. JETP **20**, 762(1965)
 - [4] M.W.Zwierlein, et al., Science **311**, 492(2006)
 - [5] G.B.Partridge, et al., Science **311**, 503(2006)
 - [6] M.W.Zwierlein, et.al., Nature **442**, 54(2006)
 - [7] Y.Shin, et.al., Phys. Rev. Lett.**97**, 030401(2006)
 - [8] C.H.Schunck, et.al., Science **316**, 867(2007)
 - [9] Y.Shin, et.al., arXiv:0709.3027
 - [10] P.F.Bedaque, et al., Phys. Rev. Lett.**91**, 247002(2003)
 - [11] T.D.Cohen, Phys. Rev. Lett.**95**, 120403(2005)
 - [12] J.Carlson and S.Reddy, Phys. Rev. Lett.**95**, 060401(2005)
 - [13] D.E.Sheehy and L.Radzihovsky, Phys. Rev. Lett. **96**, 060401(2006); Ann. Phys. (N.Y.)**322**, 1790(2007);
 - [14] C.H.Pao, et al., Phys. Rev. **B73**, 132506(2006); Z.C.Gu, et.al., arXiv:cond-mat/0603091; H.Hu and X.Liu, Phys. Rev. **A73**, 051603(R)(2006); M.Iskin and C.A.R.Sa de Melo, Phys. Rev. Lett. **97**, 100404 (2006); L.He, M.Jin and P.Zhuang, Phys.Rev.**B73**, 214527(2006); Phys.Rev.**B74**, 214516(2006)
 - [15] C.Lobo, et.al., Phys. Rev. Lett. **97**, 200403(2006)
 - [16] S.Pilati and S.Giorgini, arXiv:0710.1549
 - [17] J.Kinnunen, et.al., Phys. Rev. Lett.**96**, 110403(2006); M.Haque and H.T.C.Stoof, Phys. Rev. **A74**, 011602(2006); W.Yi and L.-M. Duan, Phys. Rev. **A73**, 031604(R)(2006); K.Machida, et.al., Phys. Rev. Lett. **97**, 120407(2006); T.N.De Silva and E.J. Mueller, Phys. Rev. **A73**, 051602(R)(2006); Phys. Rev. Lett. **97**, 070402(2006);
 - [18] Hui Hu, et.al., Phys. Rev. Lett.**98**, 070403(2007); G.Orso, Phys. Rev. Lett.**98**, 070402(2007)
 - [19] M.Randeria, J.-M. Duan and L.-Y. Shieh, Phys. Rev. Lett.**62**, 981(1989); Phys.Rev.**B41**, 327(1990)
 - [20] M.Marini, F.Pistolesi and G.C.Strinati, Eur.Phys.J.**1**, 151 (1998)[arXiv:cond-mat/9703160]
 - [21] E.Babaev and H.Kleinert, Phys.Rev.**B59**, 12083(1999); E.Babaev, Phys.Rev.**B63**, 184514(2001)
 - [22] V.M.Loktev, et al., Phys. Rept. **349**, 1(2001)
 - [23] E.Gubankova, et.al., Phys. Rev. **B74**, 064505(2006)
 - [24] For cold atom gas, the transfer can be realized in optical lattices via Raman detuning, see W.V.Liu, et.al., Phys. Rev. **A70**, 033603(2004)
 - [25] A.J.Leggett, in *Modern trends in the theory of condensed matter*, Springer-Verlag, Berlin, 1980, pp.13-27
 - [26] L.D. Landau and E.M. Lifshitz, *Quantum Mechanics. Non Relativistic Theory. Course of Theoretical Physics*, Vol. 3 (Pergamon Press, New York, 1989).
 - [27] S.Stock, et.al., Phys.Rev.Lett.**95**, 190403(2005); Z. Hadzibabic, et.al., Nature**441**, 1118(2006)
 - [28] W.Zhang, G.-D.Lin and L.-M. Duan, arXiv:0803.2488
 - [29] F.Chevy, Phys. Rev. Lett.**96**, 130401(2006); Phys. Rev. **A74**, 063628(2006); A.Bulgac and M.M.Forbes, Phys. Rev. **A75**, 031605(2007)
 - [30] T.N.De Silva and E.J. Mueller, Phys. Rev. Lett. **97**, 070402(2006); H.Caldas, J.Stat.Mech. P11012(2007)
 - [31] J.Tempere, et.al., Phys. Rev. **B75**, 184526(2007)
 - [32] D.E.Sheehy and L.Radzihovsky, Phys. Rev. **B75**, 136501(2007)
 - [33] F.Fumarola, et.al., arXiv:cond-mat/0703003